JOINT INSTITUTE FOR NUCLEAR RESEARCH
Bogoliubov Laboratory of Theoretical Physics

FINAL REPORT ON THE START PROGRAMME

“Phonon mean free path analysis in polycrystalline graphene: effect of extended defects”

Supervisor:
Dr. Sergey Krasavin

Student:
Ibrahim Abdelkader Ebied Ali,
South Valley University
(Egypt)

Participation period:
May 12 – July 06,
Winter Session 2024

Dubna, 2024

Contents

1. Abstract

The deformation potential method framework is used to study the impact of grain boundary (GB) structure, size, and shape on polycrystalline graphene's thermal conductivity. The Boren approximation yields exact analytical equations for the phonon mean free path (MFP). In the long-wavelength limit, we observed precisely two kinds of behavior: MFP acts as ω-3 for closed setups (loops) and varies as ω-1 for open GBs of any form. MFP tends to a constant value for all configurations in the short-wavelength limit. For every GB, oscillatory behavior is seen, suggesting that they behave as phonon diffraction gratings. Inherent in GBs with anomalies resulting from partial disclination dipoles is also this feature.

2. Mastering technical tools

Over the training of two months of practice, I actively mastered the wolfram mathematica programming language. learned how to work with graphs, histograms, and various equations

3. Introduction

Graphene films produced on a large-scale using CVD synthesis are generally polycrystalline. Any practical use of graphene, as in sensors and detectors, needs to consider this. In fact, it was discovered that the electrical,1 mechanical,2 and other physical properties of graphene are significantly impacted by grain boundaries (GBs).

We proposed a model of phonon scattering by a finite-length grain boundary two decades ago, based on wedge disclination dipoles (WDDs).3This model actually depends on the notion that it is more natural to characterize grain boundaries using dislinations because in certain circumstances, rotational defects rather than translational defects might define grain boundaries.4 We made use of the fact that the distant strain fields resulting from edge dislocations and WDDs accord. This enables the well-known Klemens model to be expanded to account for the boundary's finiteness.

Specifically, we discovered that when the phonon mean free path (MFP) l exhibits a crossover from l ~ ω-1 at low frequencies to a constant value with rising ω, the biaxial WDD with nonskew axis of rotation (BWDD) exhibits a highly peculiar behavior. This results in the thermal conductivity, κ, crossing over from κ ~ T2 to κ ~ T3, which is significant for explaining the sporadic low-temperature anomalies that are rarely noticed.

It is interesting that in some modern 2D polycrystalline materials like graphene and phosphorene, grain boundaries were found to be constructed of 5-7 rings or, equivalently, of 5-7 disclination dipoles.1,6 Moreover, these dipoles are nothing else but BWDDs which serve as a basic structural unit of various types of grain boundaries. Placing 5-7 BWDDs in a continuous line, one obtains a worm-like GB. A space between 5 and 7 dipoles is directly related to the misorientation angles of GBs. Thus, the problem arises of describing phonon scattering by such walls made from BWDDs. Much work in this direction has been done within molecular dynamics (MD) simulations. In particular, it has been found in equilibrium MD simulations that the thermal conductivity of ultra-fine grained graphene is one order of magnitude lower than that for pristine graphene.7 Besides, the effect of sharp temperature jump at the grain boundary was observed within non-equilibrium MD simulations.8 All MD calculations predict a decrease in thermal conductivity with a decreasing size of the grain boundary. A similar behavior was revealed using both Landauer-Büttiker9 and Boltzmann transport formalisms10 where, in addition, the significant role of individual properties of GBs was noted.

In this report, we present exact analytical results for the GB-induced phonon mean free path within the framework of BWDD’s model. The proposed calculation scheme allows us to consider any configuration of

BWDDs, both straight GBs oriented along some axis (open GB)11 and any closed GBs when 5-7 dipoles are arranged as loops in pristine graphene.12 In so doing, we mean that GB can change its direction locally.

4. Model

Considering the two-dimensional nature of phonon transport in graphene, the GB-induced MFP can be expressed as follows:15

$$l^{-1} = n_{def} \int_0^{2\pi} (1 - \cos\theta) R(\theta) d\theta, \qquad (1)$$

where ndef is the areal density of defects, θ is the scattering angle, and R(θ) is the effective differential scattering width. Here, we limit our analysis to the most significant acoustic phonon branching in the TA and LA. R(θ) in the Born approximation has the following form

$$R(\theta) = \frac{kS^2}{2\pi\hbar^2 v_\lambda^2} \overline{|\langle \mathbf{k}|U(r)|\mathbf{k}'\rangle|^2}, \qquad (2)$$

The sound velocities of the phonon branches λ (λ = TA, LA) are represented by v_λ , the projected area is S, the effective perturbation energy of a phonon due to strain fields caused by the GB is U (r), and the bar indicates an averaging procedure over α, which defines an angle between the scattering vector q = K - K′ and the axis along the GB orientation.

Assuming that the effect of strain fields leads only to a change in the velocity of sound v_λ and taking the energy of phonon with frequency ωλ(k) as $\hbar$ kv_λ, the perturbation energy is written as

$$U(r) = \hbar k v_\lambda \gamma_\lambda Tr E_{ij}^d(r). \qquad (3)$$

Here, T rE_{ij}^d(r) is the trace of the strain tensor due to GB, γ_λ is the Grüneisen constant for a given phonon branch λ, and $\hbar$ is the Planck constant. The strain field caused by GB of any size and shape can be obtained as a sum of strains of
5-7 BWDDs. The explicit expression for R (θ) is found immediately after calculating the Fourier transform of U (r) given by Eqs. (3) and (4)

$$\mathrm{Tr}E_{ij}^{d}(r)=\frac{(1-2\sigma)}{2G(1+\sigma)}\mathrm{Tr}\sigma_{ij}^{d}(r)=\frac{(1-2\sigma)}{4\pi(1-\sigma)}\left(\Omega\sum_{n=1}^{p}\ln\frac{(x-x_{n1})^2+(y-y_{n1})^2}{(x-x_{n2})^2+(y-y_{n2})^2}+\omega\ln\frac{(x-x'_{m2})^2+(y-y'_{m2})^2}{(x-x'_{m1})^2+(y-y'_{m1})^2}\right). \tag{A}$$

$$\langle\mathbf{k}|U(r)|\mathbf{k}'\rangle=\frac{1}{S}\int d^2rU(x,y)\exp\left(iq_xx+iq_yy\right)=-\frac{4\pi A}{Sq^2}\sum_{n=1}^{p}\left[\exp\left(iq_xx_{n1}\right)\exp\left(iq_yy_{n1}\right)-\exp\left(iq_xx_{n2}\right)\exp\left(iq_yy_{n2}\right)\right], \tag{4}$$

where $A=\hbar kv_\lambda\gamma_\lambda\nu(1-2\sigma)/2(1-\sigma)$, $q=|k-k'|=2k\sin(\theta/2)$, $\nu=\Omega/2\pi$, and Ω is the value of the Frank vector. Finally, after averaging $|\langle\mathbf{k}|U(r)|\mathbf{k}'\rangle|^2$ with respect to α, we obtain

$$R(\theta)=\frac{\pi A^2}{\hbar^2v_\lambda^2 4k^3\sin^4(\theta/2)}\sum_{n=1}^{p}\sum_{m=1}^{p}\{J_0\left[|2k\sin(\theta/2)\sqrt{[(x_{n1}-x_{m1})^2+(y_{n1}-y_{m1})^2]}|\right]-J_0\left[|2k\sin(\theta/2)\sqrt{[(x_{n2}-x_{m1})^2+(y_{n2}-y_{m1})^2]}|\right]$$
$$-J_0\left[|2k\sin(\theta/2)\sqrt{[(x_{n1}-x_{m2})^2+(y_{n1}-y_{m2})^2]}|\right]+J_0\left[|2k\sin(\theta/2)\sqrt{[(x_{n2}-x_{m2})^2+(y_{n2}-y_{m2})^2]}|\right]\}, \tag{5}$$

where $J_0\left[|2k\sin(\theta/2)\sqrt{[(x_{ni}-x_{mj})^2+(y_{ni}-y_{mj})^2]}|\right]$ is the Bessel function of the first kind. Accordingly, after integration over θ in Eq. (1), the phonon MFP takes the form

$$l_{GB,\lambda}^{-1}=\frac{n_{GB}v^2D^2\pi}{4k}\sum_{n=1}^{p}\sum_{m=1}^{p}[-\Im(k,x_{n2},x_{m1},y_{n2},y_{m1})-\Im(k,x_{n1},x_{m2},y_{n1},y_{m2})+\Im(k,x_{n1},x_{m1},y_{n1},y_{m1})+\Im(k,x_{n2},x_{m2},y_{n2},y_{m2})], \tag{6}$$

where $D = \gamma_\lambda(1-2\sigma)/(1-\sigma)$ and n_{GB} is the areal density of GBs. and

$$\Im(k,x_{ni},x_{mj},y_{ni},y_{mj})=-2\pi k^2\left[(x_{ni}-x_{mj})^2+(y_{ni}-y_{mj})^2\right]\left(J_0^2(k\sqrt{[(x_{ni}-x_{mj})^2+(y_{ni}-y_{mj})^2]})+J_1^2(k\sqrt{[(x_{ni}-x_{mj})^2+(y_{ni}-y_{mj})^2]})\right.$$
$$\left.-\frac{1}{k\sqrt{[(x_{ni}-x_{mj})^2+(y_{ni}-y_{mj})^2]}}J_0(k\sqrt{[(x_{ni}-x_{mj})^2+(y_{ni}-y_{mj})^2]})J_1(k\sqrt{[(x_{ni}-x_{mj})^2+(y_{ni}-y_{mj})^2]})\right).$$

4.1. Phonon mean free path

Let's evaluate the situation $p = 2$ and put dipoles at points $(x_{1i}, y_{1i}) = \left(\pm\frac{L}{2} + \delta, \frac{L}{2} \pm \delta\right), (x_{2i}, y_{2i}) = \left(\mp\frac{L}{2} - \delta, -\frac{L}{2} \mp \delta\right)$

Such an arrangement corresponds to the SW flaw. One obtains (see also Ref. 13)

$$l_{SW,\lambda}^{-1} = 2\pi^2 k n_{sw} D^2 v^2 \left[2\tilde{L}^2 \left(J_0^2(k\tilde{L}) + J_1^2(k\tilde{L}) - J_0(k\tilde{L}) J_1(k\tilde{L})/k\tilde{L} \right) \right.$$

$$\left. - \sum_{n=1}^{2} L_n^2 \left(J_0^2(\sqrt{2}kL_n) + J_1^2(\sqrt{2}kL_n) - J_0(\sqrt{2}kL_n) J_1(\sqrt{2}kL_n)/\sqrt{2}kL_n \right) \right], \tag{7}$$

where n_{SW} is the areal density of SW defects, $L^{\sim} = \sqrt{L^2 + 4\,\delta^2}$, $L_1 = L + 2\delta$, $L_2 = L - 2\delta$.

The dipole arm L and the distance between the dipoles h are the two distinctive sizes of rectilinear GBs. Possessing dipoles within points $(x_{11}, y_{11}) = (L, 0)$, $(x_{12}, y_{12}) = (0,0)$, $(x_{21}, y_{21}) = (2L + h, 0)$, $(x_{22}, y_{22}) = (L + h, 0)$,

We obtain

$$l_{GB,\lambda}^{-1} = \pi^2 k n_{GB} D^2 v^2 \left[\sum_{n=1}^{3} Z_n^2 \left(J_0^2(kZ_n) + J_1^2(kZ_n) - J_0(kZ_n) J_1(kZ_n)/kZ_n \right) \right.$$

$$\left. - 2Z_4^2 \left(J_0^2(kZ_4) + J_1^2(kZ_4) - J_0(kZ_4) J_1(kZ_4)/kZ_4 \right) \right], \tag{8}$$

where $Z_1 = \sqrt{2}L$, $Z_2 = 2L + h$, $Z_3 = h$, $Z_4 = L + h$.

5. Results

Figure 1 presents numerical results for MFPs as a function of normalized wavevector for a rectilinear arrangement of GBs, including the scenarios of point impurities and SW defects. For every kind of fault, the primary model parameters are assumed to be the same.

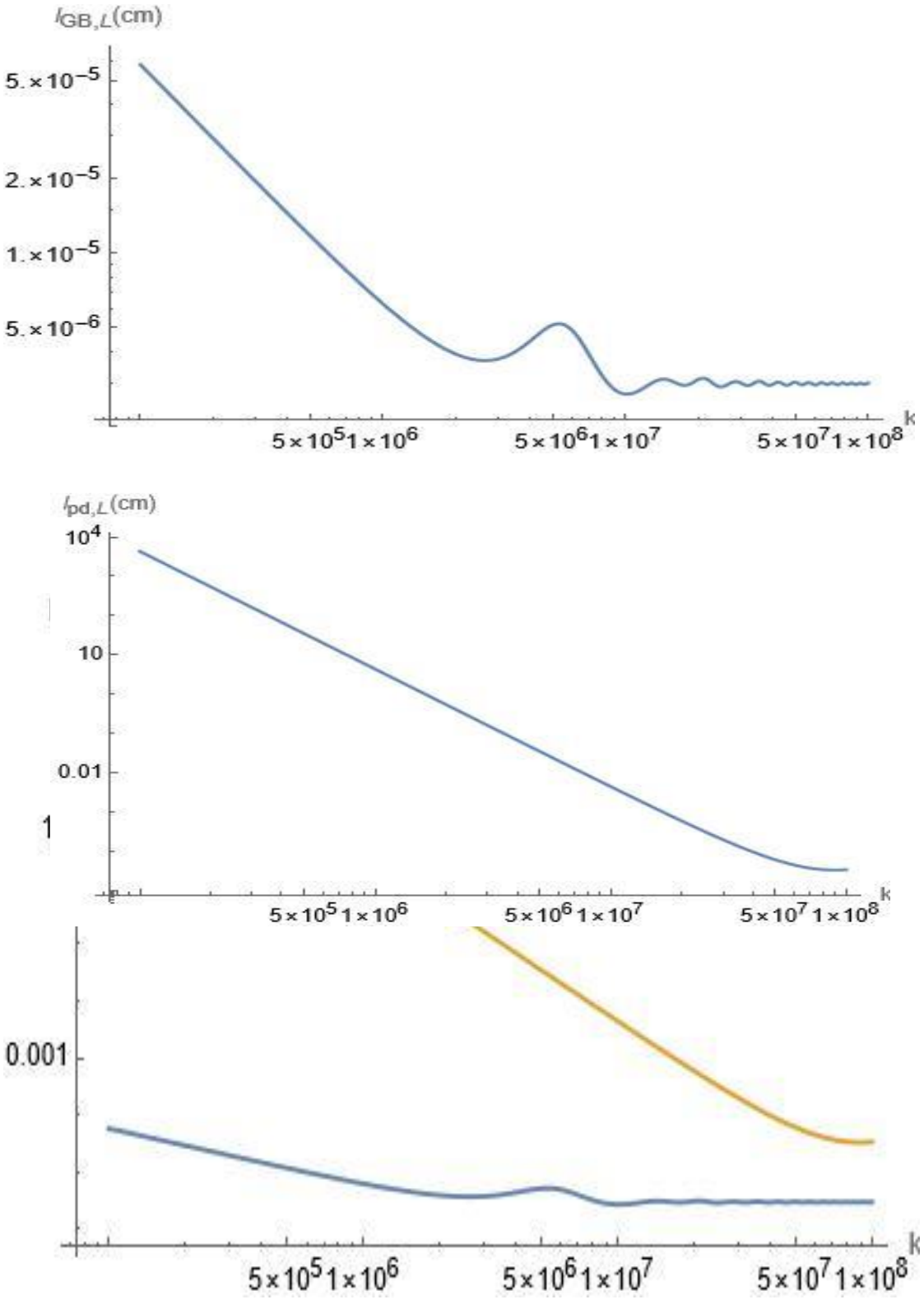

FIG. 1. The mean free paths of longitudinal phonons $l_{GB,L}$ (blue line) and as a function of wave vector (k) ,The parameter set used is: L = h = 0.24 nm, γ_{LA} = 1.7, n_{GB} = 2 x 10^{12} cm^{-2}, v = 0.16, σ = 0.16, δ = 0.04 nm. For comparison, the MFP due topoint impurity is given (red) with concentration n_{pd} = 2 x 10^{12} cm^{-2} and the model parameters taken from Ref. (13).

Specifically, any closed configuration behaves like a point impurity with ω-3. When the MFP begins to approach a constant, the crossover point at large ω is defined by the characteristic size that the loop's diameter provides. Conversely, regardless of shape, unclosed GBs always exhibit ω-1 behavior. Its physical explanation is straightforward. In fact, for every unclosed arrangement, the strain fields resulting from loops are substantially screened since they diminish as 1/r.
The crossover point's location and MFP's magnitude are the only two factors impacted by the GB's characteristic size, which is the shortest distance between end points. It is discovered that an open configuration's shape has a small impact.

GBs in graphene have an intriguing peculiarity. This is the first instance of GBs displaying an internal structure that we are aware of. Remember that walls of dislocations that are closely packed serve as a common model for GBs. The 5-7 disclination dipoles in graphene can be found at various (and occasionally sufficiently large) distances, which also establishes the misorientation angle.6, 18, 19
Short-wave phonon scattering is expected to be the internal structure's manifestation at this configuration. We performed additional study on GBs with a fixed length and varying dipole distances (i.e., varying numbers p of BWDDs in the wall) in order to shed light on this. With the grain size represented by $\mathcal{L} = pL + (p-1)h$ and all other model parameters assumed to be identical, the density of GBs is approximated as $n_{GB} = 1/\mathcal{L}^2$. Fig. 2 presents the findings.

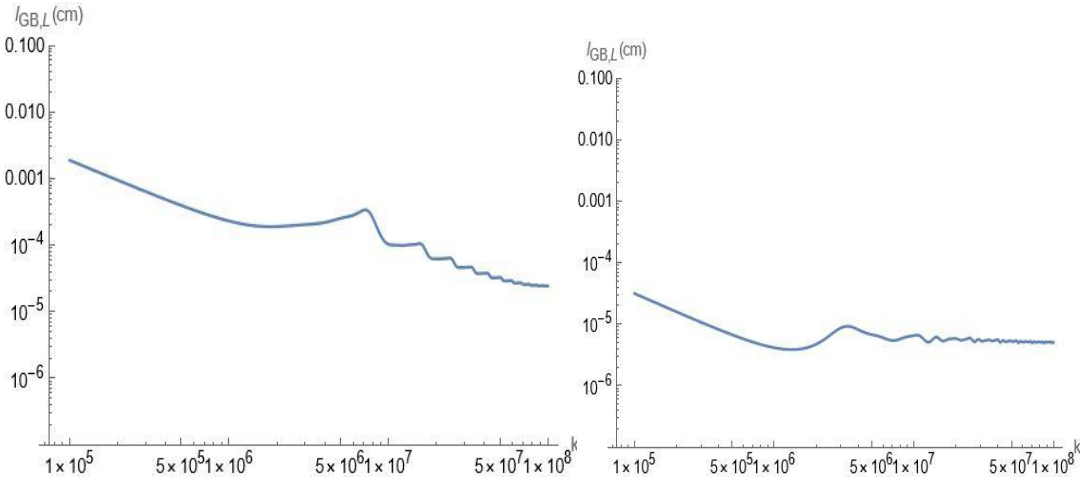

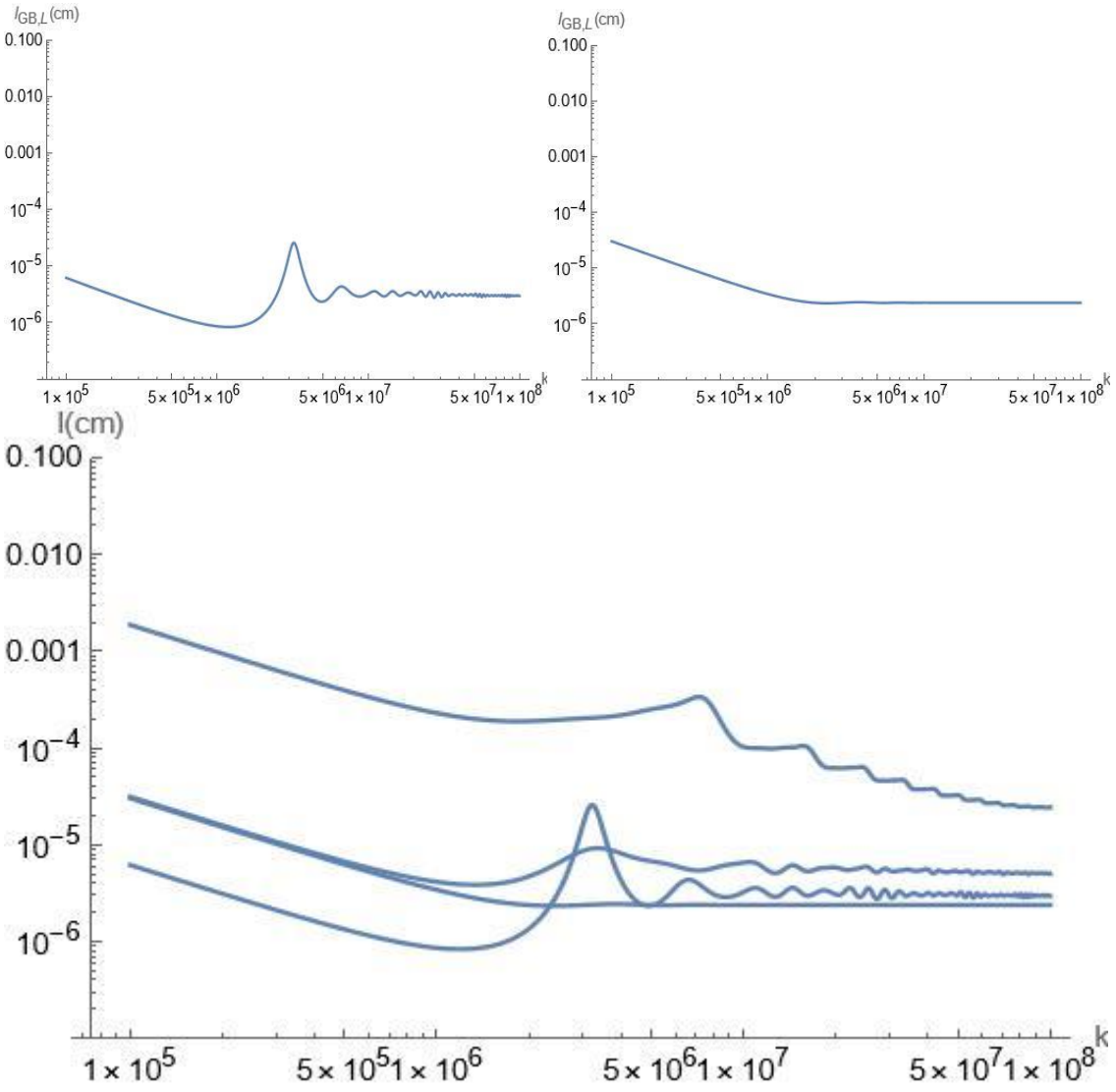

The mean free paths of longitudinal phonons lGB,L as a function of k with a fixed grain size $\mathcal{L} = 10$ nm and different distances between 5 and 7 pairs: h= 3.4 nm , h = 2 nm , h= 0.9 nm .The black line corresponds to a single dipole of 10 nm length. Other parameters are taken to be the same as in Fig. 1.

It is seen that the crossover from ω-1 to a constant behavior occurs when the phonon wavelength approaches L. Subsequently, steps in lGB(k) emerge, resulting from phonon diffraction on the wall of BWDD. In reality, the GB functions as a reciprocal lattice in k-space with a period of 1/ h, like a one-dimensional periodic grating. The procedures line up with Bragg's law. It is evident that as h increases, the value of lGB rises the wall as well becomes more transparent. In contrast, when the diffraction pattern entirely vanishes for a continuous wall with p=1, lGB gets the smallest value. It should be noted that, for a periodic arrangement of dipoles, the misorientation angle and the distance h are closely correlated (see, for example, to Ref. 25). The lower the misorientation angle, the greater the distance h. As a result, as shown in Fig. 2, the GBs with bigger misorientation angles will contribute more to the thermal conductivity.

6. Conclusion

We used the Callaway technique, which includes typical phonon processes, to theoretically analyze how GB features affect heat transfer in polycrystalline graphene. GBs have been described as rows of disclination dipoles or recurrent 5–7 topological dislocations. Most importantly, the established formalism can be used to describe GBs in any configuration. The straight GB of finite length, the Stone-Wales defect (two dipoles producing a rhombus), and straight GBs with a partial disclination dipole inside the wall—both with and without a nanocrack—have all been examined. The phonon MFP is shown to behave as follows in the longwavelength limit: it varies as ω-1 for open GBs and as ω-3 for closed configurations. The MFP is ω-independent for all GB setups for short wavelengths. We have demonstrated that, for short waves, the current internal structure of linear GBs in graphene causes a phonon diffraction at a sufficient number of 5-7 dipoles in the wall. This is evidently represented by step-like oscillations on the MFP curves (see, e.g., Fig. 2).

7. References

[1]O. V. Yazyev and S. G. Louie, Phys. Rev. B 81, 195420 (2010).
[2]R. Grantab, V. B. Shenoy, and R. S. Ruoff, Science 330, 946 (2010).
[3]V. A. Osipov and S. E. Krasavin, J. Phys. Condens. Mater. 10, L639 (1998).
[4]J. C. M. Li, Surf. Sci. 31, 12 (1972).
[5]S. E. Krasavin and V. A. Osipov, J. Phys. Condens. Mater. 13, 1023 (2001).
[6]A. E. Romanov, A. L. Kolesnikova, T. S. Orlova, I. Hussainova, V. E. Bougrov,
and R. Z. Valiev, Carbon 81, 223 (2015).
[7]B. Mortazavi, M. Pötschke, and G. Cuniberti, Nanoscale 6, 3344 (2013).
[8]A. Bagri, S. P. Kim, R. S. Ruoff, and V. B. Shenoy, Nano Lett. 11, 3917 (2011).
[9]A. Y. Serov, Z.-Y. Ong, and E. Pop, Appl. Phys. Lett. 102, 033104 (2013).
[10]Z. Aksamija and I. Knezevic, Phys. Rev. B 90, 035419 (2014).
[11]Y. Wu, Y. Hao, H. Y. Jeong, Z. Lee, S. Chen, W. Jiang, Q. Wu, R. D. Piner,
J. Kang, and R. S. Ruoff, Adv. Mater. 25, 1 (2013).
[12]E. Cockayne, G. M. Rutter, N. P. Guisinger, J. N. Crain, P. N. First, and J. A. Stroscio, Phys. Rev. B 83, 195425 (2011).
[13]S. E. Krasavin and V. A. Osipov, J. Phys. Condens. Mater. 27, 425302 (2015).
[14]J. M. Ziman, Electrons and Phonons (Clarendon Press, Oxford, 1960).
[15]J. Zhang and J. Zhao, Carbon 55, 151 (2013).
[16]V. Yu. Gertsman, A. A. Nazarov, A. E. Romanov, R. Z. Valiev, and V. I. Vladimirov, Philos. Mag. A 59, 1113 (1989).
[17]I. A. Ovid'ko, Rev. Adv. Mater. Sci. 30, 201 (2012).

8. Acknowledgement

I would like to express my gratitude to JINR for providing the opportunity to visit the START program and paying for all the necessary needs for this period and travel. In particular, I would like to thank the scientific supervisor, Dr. Sergey Krasavin for his guidance and support during our work. Also, I got all the necessary information from him that will help me implement some ideas in the future. I am also grateful to Prof. Dr. Vladimir Osipov the head of department 'Condensed matter theory' for his help and organization of my activities during this period. would also like to thank the staff of the Bogoliubov Laboratory of Theoretical Physics for the informative lectures on the research that is being conducted in the laboratory. and everyone else who helped me master all the tools in solving the problems I needed and helped me compile the programs I needed.